



**HAL**  
open science

## Understanding the removal of V, Ni and S in crude oil atmospheric residue hydrodemetallization and hydrodesulfurization

Victor Garcia-Montoto, Sylvain Verdier, Zeina Maroun, Rasmus Egeberg, Joan Tiedje, Sara Sandersen, Per Zeuthen, Brice Bouyssière

### ► To cite this version:

Victor Garcia-Montoto, Sylvain Verdier, Zeina Maroun, Rasmus Egeberg, Joan Tiedje, et al.. Understanding the removal of V, Ni and S in crude oil atmospheric residue hydrodemetallization and hydrodesulfurization. Fuel Processing Technology, 2020, 201, pp.106341. 10.1016/j.fuproc.2020.106341 . hal-02464260

**HAL Id: hal-02464260**

**<https://hal.science/hal-02464260>**

Submitted on 21 Jul 2022

**HAL** is a multi-disciplinary open access archive for the deposit and dissemination of scientific research documents, whether they are published or not. The documents may come from teaching and research institutions in France or abroad, or from public or private research centers.

L'archive ouverte pluridisciplinaire **HAL**, est destinée au dépôt et à la diffusion de documents scientifiques de niveau recherche, publiés ou non, émanant des établissements d'enseignement et de recherche français ou étrangers, des laboratoires publics ou privés.



Distributed under a Creative Commons Attribution - NonCommercial 4.0 International License

1 Understanding the removal of V, Ni and S in crude  
2 oil atmospheric residue hydrodemetallization and  
3 hydrodesulfurization

4 *Victor Garcia-Montoto<sup>a,b</sup>, Sylvain Verdier<sup>c</sup>, Zeina Maroun<sup>c</sup>, Rasmus Egeberg<sup>c</sup>, Joan L. Tiedje<sup>c</sup>,*  
5 *Sara Sandersen<sup>c</sup>, Per Zeuthen<sup>c</sup>, Brice Bouyssiere<sup>\*a</sup>*

6 <sup>a</sup>CNRS/Univ Pau & Pays Adour/E2S UPPA, Institut des Sciences Analytiques et de Physico-  
7 chimie pour l'Environnement et les Matériaux (IPREM), UMR5254, 64000, Pau, France

8 <sup>b</sup>Department of Plant and Environmental Sciences, University of Copenhagen, Thorvaldsensvej,  
9 40, Frederiksberg C, Denmark

10 <sup>c</sup>Haldor Topsoe A/S, Haldor Topsøes allé 1, 2800 Kgs. Lyngby, Denmark

11 **KEYWORDS:** Vanadium, nickel, sulfur, demetallization, desulfurization, catalysis, residue,  
12 GPC.

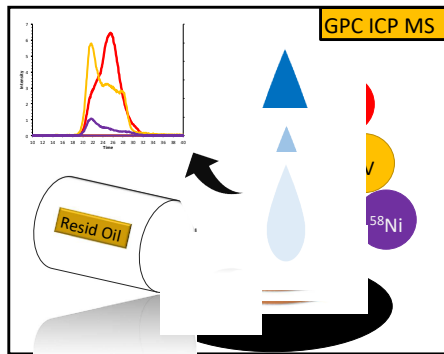
13

14 **ABSTRACT**

15 This study describes the use of gel permeation chromatography inductively coupled plasma high-  
16 resolution mass spectrometry (GPC ICP HRMS) to examine and explain two important  
17 petroleum industry catalytic processes: hydrodemetallization (HDM) and hydrodesulfurization  
18 (HDS).

19 The sulfur, nickel and vanadium species size distributions in atmospheric residue fractions were  
20 studied to track their evolution during both catalytic processes and examine their mechanisms,  
21 especially those mechanisms linked to changes in temperature and initial deactivation via coke  
22 laydown. Chromatogram shapes as well as peak areas were used to study the V, Ni and S  
23 aggregate types and concentrations in the feedstock as well as in the product after varying the  
24 operating temperature and residence time at a constant temperature. For the V and Ni  
25 compounds, the low and medium molecular weight (LMW and MMW, respectively) aggregates  
26 are easily hydrotreated under all conditions, while the high molecular weight (HMW)  
27 compounds are more refractory. For the S compounds, a different reactivity pattern was observed  
28 whereby the LMW, MMW and HMW aggregates were more similar in their reactivity, showing  
29 that the catalyst is less selective towards a certain aggregate size for the S compounds compared  
30 to the V or Ni compounds.

31 *TOC GRAPHIC*



32

### 33 INTRODUCTION

34 Hydroprocessing atmospheric residues using fixed-bed reactors is a mature technology that has  
35 been extensively studied, and close to 100 units are in operation across the globe.<sup>1</sup> Most of these  
36 units are located in Asia and the Middle East, and the total catalyst demand is estimated to be  
37 approximately 50,000 tons/year. This technology is still relevant for many refineries as it can  
38 address key issues faced by the refining industry. For example, environmental specifications are  
39 getting stricter for bunker fuels as the revised MARPOL Annex VI will reduce the sulfur cap  
40 from 3.5 to 0.5 wt% from 2020 on. Furthermore, heavier crude oils are being processed, and  
41 those feedstocks require residue technologies such as atmospheric residue desulfurization  
42 (ARDS).

43 Among the numerous elements present in crude oil, the most abundant and undesirable  
44 elements are sulfur, vanadium and nickel,<sup>2</sup> which have negative effects, such as catalyst  
45 poisoning, fouling and equipment corrosion.<sup>3,4</sup> The presence of sulfur compounds causes  
46 environmental and health problems as well, with the emission of toxic S species into the  
47 atmosphere.<sup>5,6</sup> With the purpose of reducing these undesirable effects, catalytic removal of these  
48 elements is currently carried out in the industry, especially for atmospheric and vacuum residue  
49 oils, whose content of these elements is much higher.

50 The ARDS process will be briefly described below, but various detailed reviews and their  
51 respective references can be consulted for further information about the process and its  
52 evaluation.<sup>1,7,8</sup> The process consists of downflow trickle bed reactors in series with the following  
53 catalyst loading distributed across several reactors<sup>9</sup>: large-pore guard hydrodemetallization  
54 (HDM) catalyst (whose function is to trap V, Ni and As), a smaller-pore transition catalyst  
55 combining HDM and hydrodesulfurization (HDS) activities and a third catalyst with a higher  
56 HDS activity. The deactivation mechanisms of the catalysts in such a service have also been  
57 widely studied over the years.<sup>10</sup> The initial step, which is quite rapid, is mostly due to coke  
58 formation.<sup>11</sup> This step is followed by a slower deactivation phase during which metals gradually  
59 cover the catalyst surface.<sup>12</sup> The last phase is a rapid loss of activity where the metals and coke  
60 create pore plugging or restrict access to the pore structure.

61 Many ARDS units are operated to obtain a fixed sulfur or Conradson carbon residue (CCR)  
62 content in the product. However, due to the difficult nature of the feedstock (high amount of  
63 metals and coke precursors), many challenges are encountered: short cycle length due to high  
64 deactivation rates, pressure-drop issues due to coking, demanding catalyst unloading process,  
65 long turnarounds (typically one month), etc. To minimize these issues, it is crucial that the  
66 optimal ratio between the HDM, HDM/HDS and HDS catalysts is determined for each specific  
67 ARDS unit.

68 The total amounts of Ni, V or S are an important piece of information here but do not provide  
69 any information about the nature of the molecules containing these elements. Therefore,  
70 speciation of the metals in the various feedstocks is an asset in regard to understanding the feed  
71 reactivity and the influence on the various deactivation mechanisms and ultimately in optimizing  
72 the catalyst loading. One option is to use inorganic speciation in crude oil that has been

73 developed by using size exclusion chromatography in an organic solvent linked with a high-  
74 resolution mass spectrometer working as the detector. This technique is referred to as gel  
75 permeation chromatography (GPC) and employs an organic solvent to perform the analysis, in  
76 this case tetrahydrofuran (THF).<sup>4</sup> In this technique, the compounds are separated according to  
77 their hydrodynamic volumes, which in the case of these samples follow the molecular weights of  
78 the nanoaggregates and molecules that are present in the sample. By dissolving the sample in  
79 THF, it is possible to obtain a fingerprint of the molecular distribution of the species present in  
80 the sample and evaluate how the concentrations of each fraction increase or decrease as a  
81 function of the industrial process carried out.

82 Pohl et al.<sup>13</sup> successfully used this method for two crude oils and two residue fractions and  
83 managed to map and fingerprint V, Ni, S, Fe, Co, Cr, Zn and Si. The distributions between high  
84 molecular weight (HMW) aggregates (possibly asphaltene structures), medium molecular weight  
85 (MMW) aggregates and low molecular weight (LMW) compounds (possibly free metal  
86 porphyrins and nonporphyrinic complexes) differ significantly between these samples, which  
87 will affect the HDM and HDS activities and their relative deactivation rates. Gascon et al.<sup>14</sup> used  
88 the same approach on the Saturate, Aromatic, Resin and Asphaltene (SARA) fractions of four  
89 crude oils, one atmospheric residue and one vacuum residue. The amount of each type of  
90 aggregate (HMW, MMW and LMW) was calculated, and significant variations can be observed  
91 among the four crude oils and their residue fractions. However, to understand the significance of  
92 these variations in the ARDS process, it is necessary to study not only the feedstock but also the  
93 hydrotreated product to understand the reactivity of the various types of aggregates.

94 With an increasing demand for low-sulfur fuel oil (LSFO), refineries are starting to consider  
95 alternative usages for their ARDS units, for example, by coprocessing vacuum residues, which

96 are typically processed in ebullated bed reactors due to the high amount of metals and  
97 asphaltenes in this type of feed, which causes an extremely rapid deactivation of the catalyst. A  
98 feedstock change often requires changing the operating conditions in the unit (e.g., by lowering  
99 the feed rate to lower the liquid hourly space velocity) and redesigning the catalyst loading. The  
100 latter is not always straightforward, as it requires a very thorough understanding of the feed and  
101 its effect on the catalyst activity throughout the entire cycle to avoid untimely shutdowns. To this  
102 end, a better understanding of not only the feed properties (contents of sulfur, nitrogen,  
103 asphaltene, etc.) but also the molecular composition is invaluable. Thus, in this paper, two ARDS  
104 pilot plant studies are reported. In study A, the temperature was adjusted from 375 to 385 °C to  
105 evaluate its influence on the reactivity of the various sulfur, nickel and vanadium species. In  
106 study B, the fate of sulfur, nickel and vanadium nanoaggregates was monitored under constant  
107 operating conditions to examine the role of the initial coke laydown on the HDM and HDS  
108 reactions.

## 109 **MATERIALS AND METHODS**

### 110 **Instrumentation**

111 A quantitative analysis of all the feedstocks was carried out with the purpose of determining  
112 the mass variations of the target elements by using inductively coupled plasma mass  
113 spectrometry (ICP-MS). The principle of the method is to determine the total amount of xylene-  
114 soluble Ni and V compounds with inductively coupled plasma mass spectrometry (ICP-MS) after  
115 suitable dilution of the petroleum/petroleum product sample by weight with xylene. The  
116 vanadium and nickel contents are quantified by ICP-MS using a vanadium-isotope mass of 51  
117 and a nickel-isotope mass of 60 through comparison with calibration curves obtained via 500 wt  
118 ppm Conostan organometallic V and Ni standards diluted with xylene. Scandium is used as an

119 internal standard to correct for drift and matrix effects. The removal of molecular interferences in  
120 the ICP-MS analysis was performed with helium kinetic energy discrimination. EnviroMAT  
121 used-oil matrix reference material containing V and Ni was analyzed with each sample batch to  
122 monitor the analysis accuracy. The physico-chemical properties of the feeds and products were  
123 measured using the following standard methods: Nitrogen (ASTM D5762), Sulfur (ASTM D  
124 4294, Hydrogen (ASTM D 7171 H), asphaltene (ASTM D6560), microcarbon residue (MCR)  
125 (ASTM D4530), specific gravity (SG) (ASTM D4052), and simulated distillation (ASTM  
126 D7169). Carbon (wt %) content was calculated by difference with 100% with N, S and H  
127 content.

128 All the speciation analyses were carried out with a Thermo Scientific Element XR double  
129 focusing sector field ICP-MS (Thermo Fisher, Germany) instrument accessing the spectrally  
130 interfered isotopes of  $^{32}\text{S}$ ,  $^{51}\text{V}$  and  $^{58}\text{Ni}$  at a resolution of 4,000 (medium resolution). The mass  
131 spectrometer was equipped with a quartz injector (1.0 mm inner diameter (i.d.)), a Pt sampler  
132 cone (1.1 mm orifice diameter) and a Pt skimmer cone (0.8 mm orifice diameter). An  $\text{O}_2$  gas  
133 flow of 0.08 mL/min was included to avoid carbon deposition. Both the instrument and mass  
134 calibration settings were optimized daily at resolutions of 300 (low resolution) and 4,000. A  
135 medium resolution avoids the spectral interference of  $\text{O}_2$  on the  $^{32}\text{S}$  isotope. These optimizations  
136 were carried out using a tuning solution containing 1.0 ng g<sup>-1</sup> of Ag, Al, B, Ba, Ca, Cd, Co, Cr,  
137 Cu, Fe, In, K, Li, Mg, Mn, Mo, Na, Ni, P, Pb, Sc, Si, Sn, Ti, V, Zn and Y in tetrahydrofuran  
138 (THF). A mass offset was also applied to compensate for the mass drift coming from the sector  
139 field magnet.<sup>15,16</sup>

140 The mass spectrometer was equipped with a modified DS-5 microflow total consumption  
141 nebulizer (CETAC, Omaha, NE) mounted with a laboratory-made jacketed spray chamber



142 heated to 60 °C by a water/glycol mixture working with a temperature-controller bath circulator  
143 Neslab RTE-111 (Thermo Fisher Scientific, Waltham, MA).<sup>17</sup>

144 The chromatographic separation was carried out using three Waters (Waters Corporation,  
145 Milford, MA) styrene-divinylbenzene gel permeation columns (7.8 mm i.d. and 300 mm length).  
146 These three columns included an HR4 column (particle size of 5 µm with an exclusion limit of  
147 600,000 Da of polystyrene equivalent), an HR2 column (particle size of 5 µm with an exclusion  
148 limit of 20,000 Da) and an HR0.5 column (particle size of 5 µm and an exclusion limit of 1,000  
149 Da of polystyrene equivalent). A Dionex high-performance liquid chromatography (HPLC)  
150 system fitted with an UltiMate 3,000 microflow pump, an UltiMate 3,000 autosampler and a low  
151 port-to-port dead-volume microinjection valve were used to deliver the carrier solution and  
152 mobile phase. To prevent possible damage to the GPC columns, a Styragel guard column (4.6  
153 mm i.d. and 30 mm length) was also fitted between the columns and the pumping system.

154 **Methodology.** One feed, which is a blend of 93% of atmospheric residue (ATM) and 7%  
155 vacuum residue (VAC), was hydrotreated under different conditions for the purpose of  
156 evaluating and understanding the removal of the target compounds by applying the method  
157 optimized by Desprez et al.<sup>16</sup> and Vargas et al.<sup>18</sup>. These researchers studied the size distributions  
158 of V, Ni and S and established the integration intervals for HMW, MMW and LMW aggregates  
159 in crude oil as follows: 1,100-1,400 s (18 – 23 mL of eluted sample) for HMW compounds,  
160 1,400-1,600 s (23 – 27 mL) for MMW compounds and above 1,600 s (< 27 mL) for LMW  
161 compounds. The comparison of the different sizes of species will provide useful information  
162 about the removal of target compounds.

163 In addition, with the purpose of monitoring the stability of the ICP HR MS intensities, analysis  
164 of known crude oil samples, whose composition had been studied previously, was periodically  
165 carried out.

166 **Reagents, samples and solutions.** Tetrahydrofuran, multisolvent GPC grade, ACS, stabilized  
167 with 250 ppm of butylated hydroxytoluene (BHT) (Scharlau, Spain) to prevent the formation of  
168 peroxides, was used both for sample preparation and for chromatographic elution.

169 All the atmospheric residue crude oil feeds were provided by Haldor Topsoe (Denmark), and  
170 the feeds were analyzed by diluting them in THF at dilution factors of 50 for the 93% ATM/7%  
171 VAC feed blend and of 5 for the products.

172 **Pilot plant testing.** The pilot tests were performed in a once-through downflow trickle bed  
173 pilot plant located in Haldor Topsoe's R&D facilities. The unit consists of two reactors in series.  
174 The product was first separated in a high-pressure separator (HPS). The liquid product from the  
175 HPS was sent to a low-pressure separator (LPS) and to a stripper for removal of gases and other  
176 noncondensed light hydrocarbons. Nitrogen was used as the stripping agent, and once-through  
177 pure hydrogen was used. The catalyst was diluted with an inert material (mesh 60 carborundum)  
178 using a 25 vol% SiC/75 vol% catalyst ratio. The operating conditions are given in Table 1 for  
179 study A (influence of the temperature) and study B (influence of the initial deactivation). The  
180 feed properties are listed in Table 2. The results of study A are summarized in Table 3, and the  
181 results of study B are provided in Table 4. Note that the catalysts loaded were commercial  
182 catalysts used in residue service developed and produced by Haldor Topsoe A/S.

183

184 **Table 1.** Operating Conditions of the Pilot Plant Tests

Inlet pressure hydrogen (barg)	165
H <sub>2</sub> /oil (mL/L)	550
Overall liquid hourly space	0.2

velocity (LHSV) (h <sup>-1</sup> )	
------------------------------------	--

185  
186  
187  
188  
189  
190  
191  
192

**Table 2. Feed Properties**

Property	Method	Atmospheric residue (ATM)	Vacuum residue (VAC)	Blend 93 vol% ATM and 7 vol% VAC
Nitrogen, wt ppm	D 5762	2800	4500	3100
Sulfur, wt%	D 4294	3.985	5.00	4.061
Hydrogen, wt%	D 7171 H	10.75	(11.18)*	10.78
C, wt%	By difference	85.0	83.4	84.8
H/C	-	0.13	0.13	0.13
SG 60/60 °F	D 4052	0.9797	-	0.9847
Density at 40 °C, g/ml	D 4052	0.9621	-	0.9672
Nickel, wt ppm	ICP-MS	21.1	42.4	27.0
Vanadium, wt ppm	ICP-MS	61.1	121	73.0
Carbon Residue, wt%	D 4530	12.02	24.42	12.96
Asphaltenes, wt%	D 6560	5.1	11.0	6.4
Simulated Distillation	D 7169			
0.5 wt% (IBP), °C		221	415	235
5 wt%, °C		341	515	353
10 wt%, °C		378	542	388
30 wt%, °C		454	600	467
50 wt%, °C		535	649	546
70 wt%, °C		614	709	627
80 wt%, °C		665	-	676
85 wt%, °C		698	-	705
90 wt%, °C		736	-	-
95 wt%, °C		-	-	-
99.5 wt% (FBP), °C		-	-	-

193 *\*: H content back-calculated from the properties of the atmospheric residue and of the blend assuming that volume*  
194 *and weight fractions are equivalent as density could not be measured for the vacuum residue.*

195

196  
 197  
 198  
 199  
 200  
 201  
 202  
 203  
 204

**Table 3. Results of Study A (Influence of the Temperature)**

Sample type		Feed	Product	Product	Product
Run time, hours			1,003	1,101	1,337
Temperature of the reactor, °C			375	380	385
Sulfur, wt%	ASTM D4294	4.061	0.446	0.349	0.291
Nickel, wt ppm	ICP-MS	27	5.16	4.12	3.62
Vanadium, wt ppm	ICP-MS	73	8.61	6.65	5.85
Asphaltenes, wt%	ASTM D6560	6.4	1.4	1.2	1.6
Simulated Distillation	ASTM D7169				
0.5 wt% (IBP), °C		235	142	142	128
5 wt%, °C		353	258	244	234
10 wt%, °C		388	306	295	285
30 wt%, °C		467	399	391	394
50 wt%, °C		546	466	456	464
70 wt%, °C		627	541	532	542
80 wt%, °C		676	579	572	586
85 wt%, °C		705	603	595	612
90 wt%, °C		-	630	623	641
95 wt%, °C		-	665	658	678
99.5 wt% (FBP), °C		-	721	721	717

205  
 206  
 207  
 208

209  
210  
211  
212  
213  
214  
215  
216  
217

**Table 4.** Results of Study B (Influence of the Initial Deactivation Due to Coke Laydown)

Sample type		Feed	Product	Product	Product	Product
Run time, hours			23	52	76	100
Temperature of the reactor, °C			375	375	375	375
Sulfur, wt%	ASTM D4294	4.061	0.098	0.179	0.212	0.282
Nickel, wt ppm	ICP-MS	27	1.18	1.74	2.08	2.89
Vanadium, wt ppm	ICP-MS	73	2.02	2.84	3.25	4.32
Simulated Distillation	ASTM D7169					
0.5 wt% (IBP), °C		235	142	67	142	155
5 wt%, °C		353	249	247	260	272
10 wt%, °C		388	301	300	313	323
30 wt%, °C		467	407	403	415	421
50 wt%, °C		546	482	474	491	497
70 wt%, °C		627	572	553	577	583
80 wt%, °C		676	632	598	632	639
85 wt%, °C		705	675	626	668	676
90 wt%, °C		-	-	659	716	721
95 wt%, °C		-	-	702	-	-
99.5 wt% (FBP), °C		-	-	-	-	-

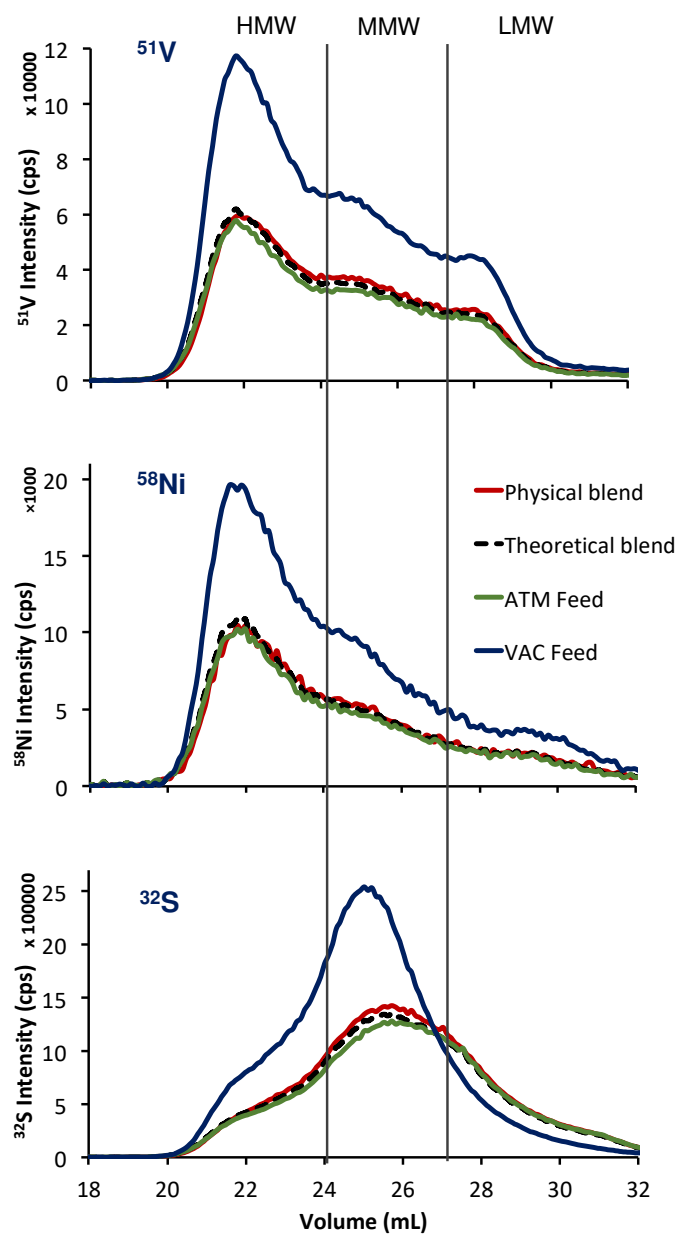
218  
219  
220  
221

## RESULTS AND DISCUSSION

### Feedstock properties and fingerprints of the metal complexes in the feedstocks

222 The physico-chemical properties of the atmospheric and vacuum residues as well as those of  
223 the blends are listed in Table 2. The properties are in line with those of the typical atmospheric  
224 and vacuum residues reported in the literature.<sup>1</sup> It is interesting to note that there is a factor of 2  
225 difference between the two residues with respect to the Ni, V, asphaltene and MCR contents.

226 When two feeds are blended, it is important to check whether aggregation phenomena occur as  
227 these aggregates may influence the asphaltene stability and thereby the residue hydrotreating  
228 process. As shown in Figure 1, the theoretical blend (i.e., the calculated profile based on the  
229 analysis of the atmospheric and vacuum residues) and the physical blend show the same  
230 distribution, indicating that no nanoaggregation occurs. It should be noted that this finding could  
231 be a consequence of the fractions stemming from the same crude oil. Indeed, trimodal size  
232 distributions are observed for both the V and Ni compounds present in these feedstocks, while a  
233 less pronounced trimodal distribution, much richer in MMW aggregates, is observed for the  
234 sulfur compounds.



235

236 **Figure 1.** GPC ICP HR MS chromatograms of the V, Ni and S species in the atmospheric residue feedstock (ATM, green line),  
 237 vacuum residue (VAC, blue line), blend of 93 vol% ATM and 7% VAC (physical blend, red line) and theoretically reconstructed  
 238 blend of 93 vol% ATM and 7 vol% VAC (black dashed line) based on individual ATM and VAC chromatograms.

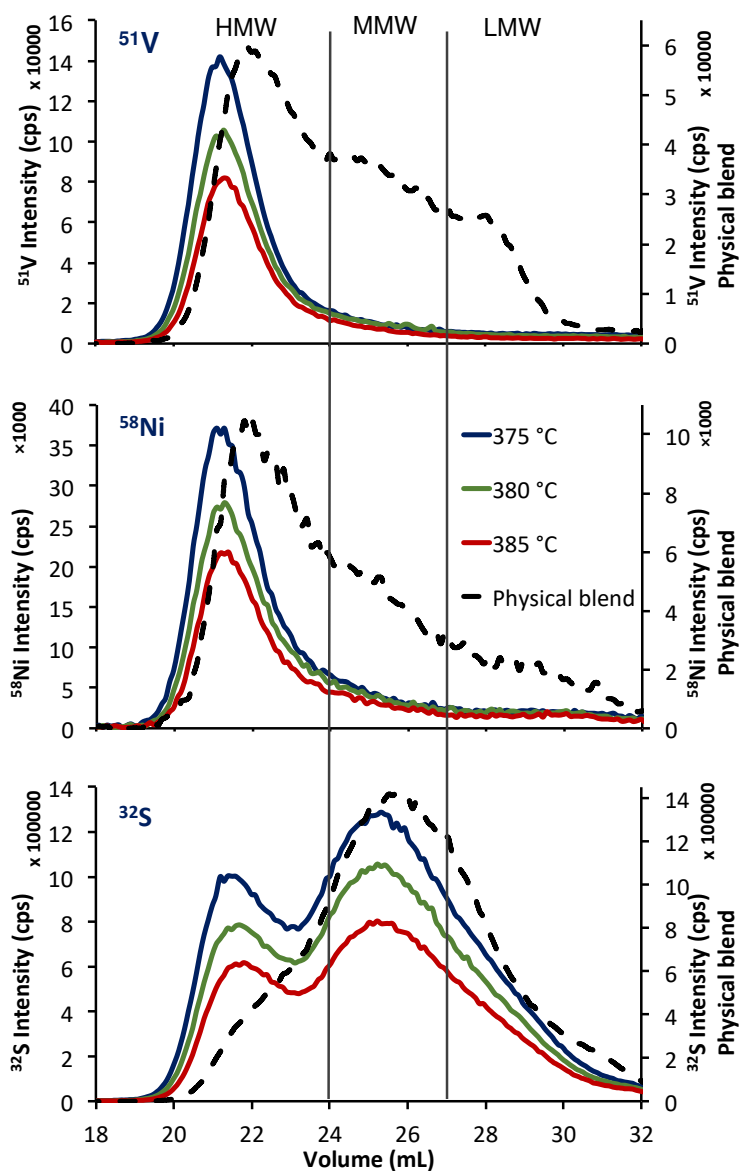
239

240 The size distributions of different crude oils and residues were studied elsewhere,<sup>14</sup> showing  
 241 the presence of HMW, MMW and LMW nanoaggregates, and the HMW compounds were the

242 most abundant in Ni and V, while the MMW nanoaggregates were most abundant in S. The  
243 results obtained in this study are consistent with these previous results.

#### 244 Study A – influence of the temperature

245 *Behavior of V and Ni.* The evolution of the V and Ni species present in the feed after having  
246 been through the hydrotreating process at different temperatures has been studied. The samples  
247 were hydrotreated at the three different temperatures previously mentioned: 375 °C, 380 °C and  
248 385 °C.



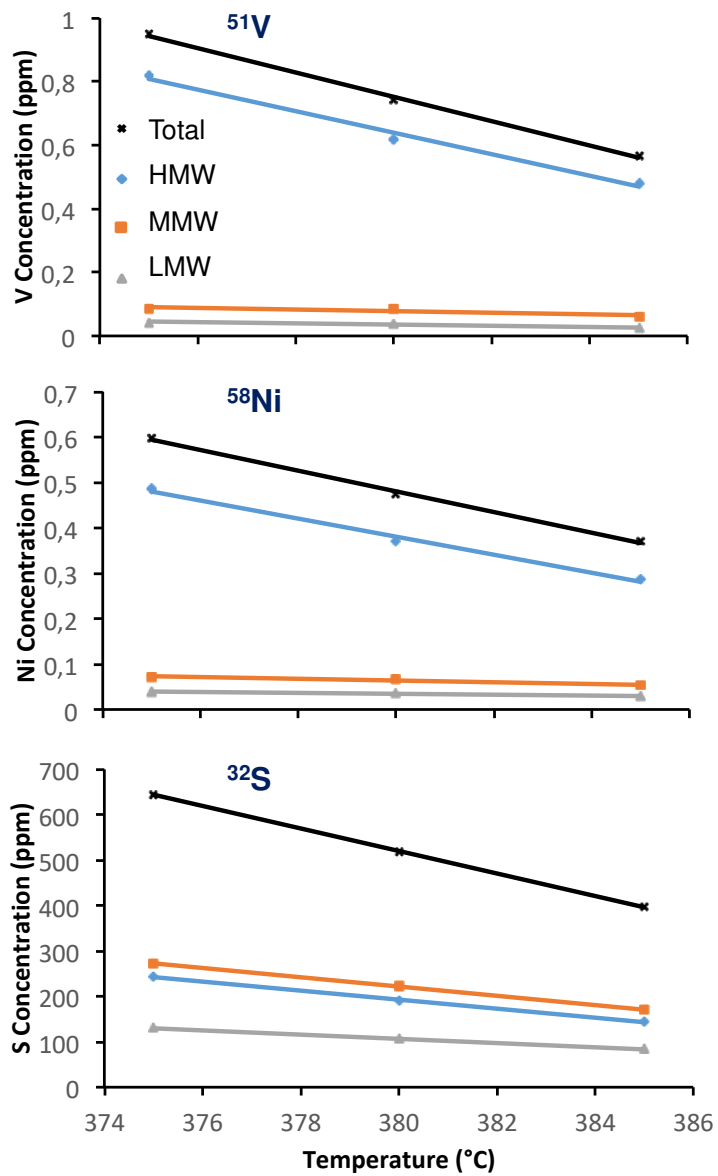
249



250 *Figure 2. GPC ICP HR MS chromatograms of the V, Ni and S species in the feed (black dashed line) and the product after having*  
251 *been hydrotreated at different temperatures (the hydrotreatments at 375 °C, 380 °C and 385 °C correspond to the blue, green*  
252 *and red lines, respectively).*

253

254 Figure 2 shows that, as expected, at higher temperatures, more V, Ni and S species are  
255 removed. For V and Ni, the LMW and MMW aggregates are easily hydrotreated even at low  
256 temperatures, and as the temperature is increased, only the remaining HMW aggregates are  
257 hydrotreated. This phenomenon can be quantitatively observed in Figure 3, where the  
258 concentration of each nanoaggregate size is determined based on the areas of the peaks (details  
259 of the integration method are available in the open literature).<sup>15</sup> The concentration of LMW and  
260 MMW aggregates is negligibly small at all temperatures, while the concentration of HMW  
261 aggregates shows a linear decrease as a function of the temperature. The correlation coefficient  
262 of the slope is better for the regression of the HMW nanoaggregates compared to those of the  
263 MMW and LMW nanoaggregates, confirming that the temperature is driving the HMW  
264 hydrotreatment. From the slopes of these linear trends, as listed in Table 5, it can be readily  
265 observed that the HMW V aggregates are hydrotreated faster than the Ni aggregates. This  
266 observation is in agreement with previous results in the open literature.<sup>19</sup>



267

268 **Figure 3.** The concentrations of V, Ni and S (total in black, HMW in blue, MMW in orange and LMW in gray) in the products that  
 269 were hydrotreated at different temperatures quantified based on the total concentration and the GPC ICP HR MS  
 270 chromatograms.

271

272

273

274

275

276 **Table 5.** Slopes and Regression Coefficients for the Variation in V, Ni and S Concentrations vs. Temperature

	Total		HMW		MMW		LMW	
	Slope	r <sup>2</sup>	Slope	r <sup>2</sup>	Slope	r <sup>2</sup>	Slope	r <sup>2</sup>
V	-3.82 E-02	0.998	-3.39 E-02	0.988	-0.25 E -02	0.733	-0.19 E -02	0,965
Ni	-2.28 E-02	0.998	-1.98 E -02	0.992	-0.19 E -02	0.957	-0.10 E -02	0,879
S	-24.84	0.999	-9.955	0.997	-10.21	0.999	-4.678	0,999

277

278

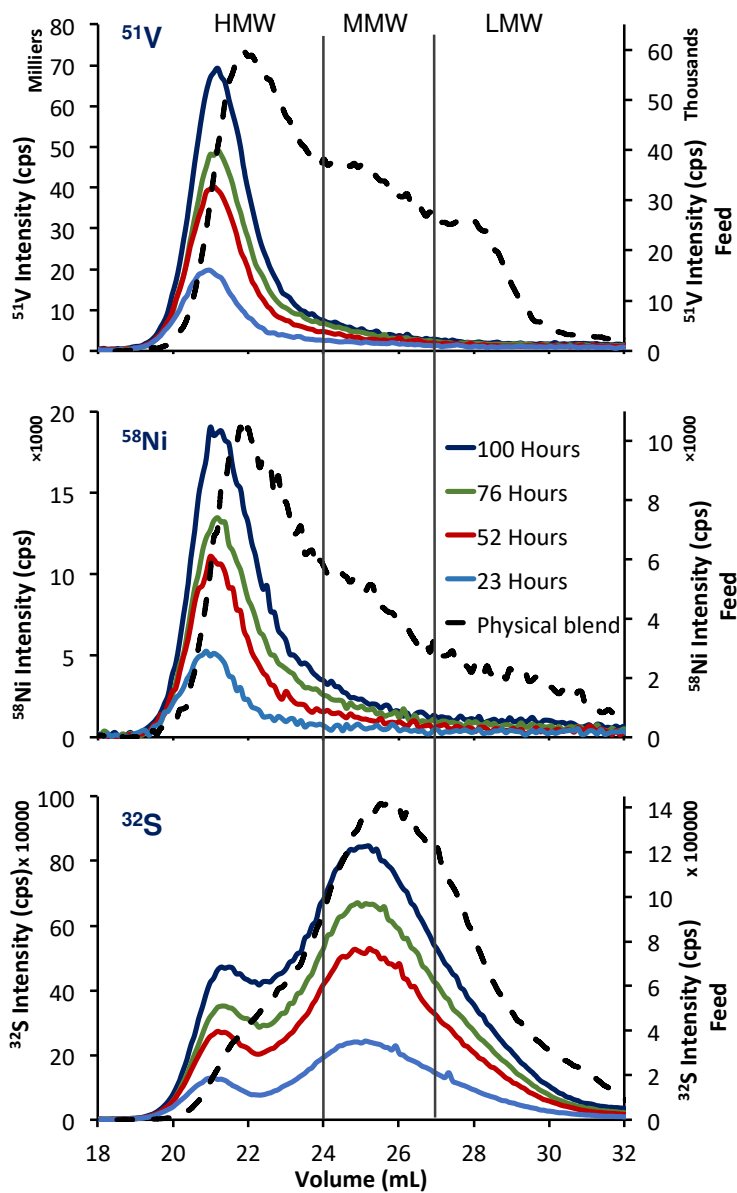
279 **Behavior of S.** Interestingly, the fate of the S aggregates differs from that observed for the V  
 280 and Ni aggregates. Figures 2 and 3 show that the LMW and MMW S aggregates are not fully  
 281 hydrotreated at the lowest temperatures. This phenomenon indicates that these LMW and MMW  
 282 compounds are more refractory compared to the size-similar V and Ni compounds. It is also  
 283 worth noting that a bimodal HMW-MMW S distribution is observed in the hydrotreated  
 284 products, while this distribution was not clearly present in the feedstock. It is likely that a  
 285 trimodal distribution occurs in the feedstock but is hidden due to the high concentration of  
 286 aggregates eluting in the MMW range. These results show that S compounds/nanoaggregates  
 287 with molecular weights between HMW and MMW are more easily removed, indicating that the  
 288 catalyst possesses a higher efficiency for these kinds of nanoaggregates.

### 289 **Study B - initial deactivation due to coke laydown**

290 The initial and fast deactivation during ARDS tests is due to coking and, more specifically, the  
 291 strong initial adsorption of polyaromatic compounds, including N-containing molecules onto the  
 292 surface of the catalyst.<sup>11</sup> In commercial units, the impact of the initial coke laydown on HDS and  
 293 HDM is not simple to evaluate. For some units, it is clear that the HDM activity is more affected  
 294 than the HDS activity during the first hundred hours. For other units, the initial deactivations of

295 the HDS and HDM activities are equal, which depends on the catalyst loading, feed properties  
296 and operating conditions. Therefore, the goal of this study was to evaluate how the initial  
297 deactivation (which is due to coke laydown) affected the hydrotreatment rates of the various  
298 aggregates and if certain differences between the initial deactivations of HDM and HDS could be  
299 observed, which could be related to the aggregate distribution. For this purpose, the temperature  
300 of the process was kept constant at 375 °C to evaluate the changes due to the initial catalyst  
301 deactivation (at 23, 52, 76 and 100 run hours).

302 ***Behavior of V and Ni.*** The evolution of the V and Ni species present in the feed after having  
303 been through the hydrotreating process at different times has been studied. As shown in Figure 4,  
304 initially, the concentration of V and Ni species is very low, but during the first hours of the test, a  
305 steady increase in the total concentration of V and N is observed. Figure 5 shows the quantitative  
306 description of this increase. This increase is almost entirely ascribed to an increase in the HMW  
307 fraction. It should be noted that most of the LMW and MMW aggregates are removed  
308 throughout the test despite the increasing deactivation (Table 6) of the catalyst, as indicated by  
309 the total product Ni and V contents listed in Table 4.



310

311 **Figure 4.** GPC ICP HR MS chromatograms of the V, Ni and S species in the feed (black dashed line) and the product for different  
 312 run times after having been hydrotreated at the same temperature (the run times of 23 h, 52 h, 76 h and 100 h correspond to  
 313 the light blue, red, green and blue lines, respectively).

314

315

316

317

318

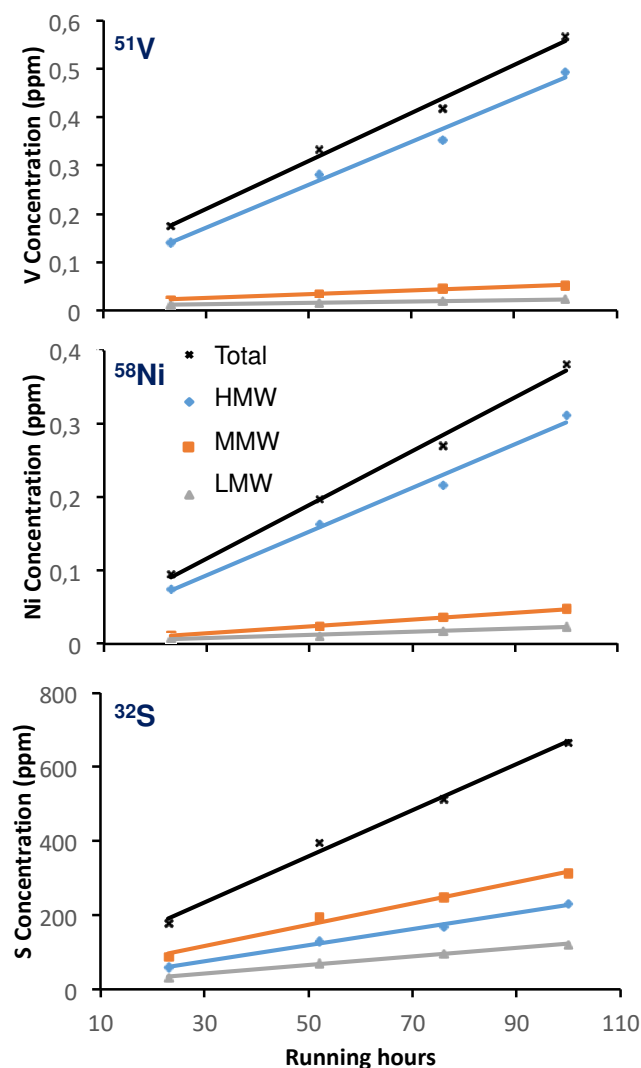
319 **Table 6.** Slopes and Regression Coefficients for the Variation in V, Ni and S Concentration vs. Run Time (Hours).

	Total		HMW		MMW		LMW	
	Slope	r <sup>2</sup>	Slope	r <sup>2</sup>	Slope	r <sup>2</sup>	Slope	r <sup>2</sup>
V	4.96 E-03	0.991	4.44 E-03	0.987	0.38 E -03	0.989	0.14 E -03	0,997
Ni	3.66 E-03	0.993	2.98 E -03	0.989	0.46 E -03	0.997	0.22 E -03	0,966
S	6,22	0.994	2.19	0.994	2.87	0.990	1.16	0,995

320

321

322 **Behavior of S.** In Figure 4, it is observed that the sulfur species follow a different evolution. A  
323 bimodal distribution of the HMW and MMW peaks is observed, and its ratio has been calculated,  
324 resulting in an almost constant value. As shown more clearly in Figure 5, the increase in S  
325 species is similar for the three groups of hydrodynamic volume distributions, which could  
326 indicate either a higher preference of the catalyst for the HMW species (if we compare the  
327 behavior of S with the behavior of V and Ni) or a more refractory behavior from the S species  
328 with the catalyst.



329

330 *Figure 5. The concentrations of V, Ni and S (total in black, HMW in blue, MMW in orange and LMW in gray) in the products that*  
 331 *were hydrotreated for different run times quantified based on the total concentration and the GPC ICP HR MS chromatograms.*

332

### 333 CONCLUSION

334 This study has provided innovative and valuable information related to the size distributions of  
 335 the different species present in atmospheric residue feedstocks and how these distributions vary  
 336 during HDS and HDM processes. Obtaining fingerprints of the metal aggregates in these  
 337 feedstocks has provided us with a better understanding of their speciation in S, Ni and V. For the

338 Ni and V aggregates, it was found that the HMW compounds are more refractory compared to  
339 the LMW and MMW compounds, which are removed at low temperatures or even after long run  
340 hours.

341 For the S aggregates, a slightly different behavior was observed whereby the LMW and MMW  
342 aggregates are not as easily hydrotreated, and in fact, the MMW nanoaggregates/compounds are  
343 slightly less easily hydrotreated compared to the HMW aggregates. This phenomenon illustrates  
344 the inherent difference in chemical composition of the metallo-organic compounds compared to  
345 the sulfur-containing compounds and their reactivity. In a previous study<sup>15,20,21</sup> free porphyrinic  
346 compounds were easily removed, possibly via easy access of the molecules to the catalyzer. Of  
347 the HMW nanoaggregate part, only a small portion can be easily removed, which can be the  
348 porphyrins linked at the surface of the nanoaggregates,<sup>15</sup> but the Ni and V compounds that are  
349 located deeper in the nanoaggregates are more difficult to remove as the shell of the  
350 nanoaggregates has to be removed first before the V and Ni compounds can access the catalyst.  
351 In regard to the S compounds, the observed behavior seems to me driven more by the types of S  
352 compounds than by the aggregation states of the S compounds. Here, the molecular  
353 conformation of the S compounds needs to be studied. More in-depth molecular studies have to  
354 be conducted.

355 Nevertheless, this study provides insights into the catalyst preference towards these  
356 compounds/nanoaggregates, which is an important factor for future optimization of the balance  
357 between the HDM and HDS catalysts for those ARDS units processing different feedstocks with  
358 different V, Ni and S nanoaggregate distributions.

359 AUTHOR INFORMATION

360 **Corresponding Author**



361 Brice Bouyssiere: brice.bouyssiere@univ-pau.fr

362 **Funding Sources**

363 **Notes**

364 **The authors declare no competing financial interest.**

365 **ACKNOWLEDGMENT**

366 Financial support from the Conseil Régional d'Aquitaine (20071303002PFM) and FEDER  
367 (31486/08011464) is acknowledged

368 **REFERENCES**

- 369 (1) Raybaud, P.; Toulhoat, H. Catalysis by transition metal sulphides.  
370 <http://www.editionstechnip.com/fr/catalogue-detail/1176/catalysis-by-transition-metal->  
371 [sulphides.html](http://www.editionstechnip.com/fr/catalogue-detail/1176/catalysis-by-transition-metal-sulphides.html) (accessed Jul 12, 2018).
- 372 (2) Ali, M.; Abbas, S. A review of methods for the demetallization of residual fuel oils. *Fuel*  
373 *Process. Technol.* **2006**, *87*, 573–584.
- 374 (3) Reynolds, J. G.; Biggs, W. R.; Bezman, S. A. Reaction sequence of metalloporphyrins  
375 during heavy residuum upgrading. In *Metal Complexes in Fossil Fuels*; Filby, R. H., Branthaver,  
376 J. F., Eds.; American Chemical Society: Washington, DC, 1987; pp 205–219.
- 377 (4) Caumette, G.; Lienemann, C.-P.; Merdrignac, I.; Bouyssiére, B.; Lobinski, R. Element  
378 speciation analysis of petroleum and related materials. *J. Anal. At. Spectrom.* **2009**, *24* (3), 263–  
379 276.
- 380 (5) Yépez, O. Influence of different sulfur compounds on corrosion due to naphthenic acid.  
381 *Fuel* **2005**, *84* (1), 97–104.
- 382 (6) Vorapalawut, N.; Labrador, M. M.; Pohl, P.; Caetano, M.; Chirinos, J.; Arnaudguilhem, C.;  
383 Bouyssiére, B.; Shiowatana, J.; Lobinski, R. Application of TLC and LA ICP SF MS for  
384 speciation of S, Ni and V in petroleum samples. *Talanta* **2012**, *97*, 574–578.
- 385 (7) Rana, M. S.; Sámano, V.; Ancheyta, J.; Diaz, J. A. I. A review of recent advances on  
386 process technologies for upgrading of heavy oils and residua. *Fuel* **2007**, *86* (9), 1216–1231.
- 387 (8) Sahu, R.; Song, B. J.; Im, J. S.; Jeon, Y.-P.; Lee, C. W. A review of recent advances in  
388 catalytic hydrocracking of heavy residues. *J. Ind. Eng. Chem.* **2015**, *27*, 12–24.

- 389 (9) Bartholdy, J.; Cooper, B. H. Optimizing hydrotreater catalyst loadings for the upgrading of  
390 atmospheric residues. In *Studies in Surface Science and Catalysis*; Absi-Halabi, M., Beshara, J.,  
391 Stanislaus, A., Eds.; Elsevier: Amsterdam, 1996; pp 117–124.
- 392 (10) Bartholdy, J. Z. P.; Cooper, B. H. *The Interplay of Coke and Metals in Resid Deactivation*.  
393 Atlanta, 1994.
- 394 (11) Zeuthen, P.; Bartholdy, J.; Wiwel, P.; Cooper, B. H. Formation of coke on hydrotreating  
395 catalysts and its effect on activity. In *Studies in Surface Science and Catalysis*; Delmon, B.,  
396 Froment, G. F., Eds.; Elsevier: Amsterdam, 1994; pp 199–206.
- 397 (12) Bartholdy, J.; Hannerup, P. N. Hydrodemetallization in resid hydroprocessing. In *Studies*  
398 *in Surface Science and Catalysis*; Bartholomew, C. H., Butt, J. B., Eds.; Elsevier, 1991; pp 273–  
399 280.
- 400 (13) Pohl, P.; Dural, J.; Vorapalawut, N.; Merdrignac, I.; Lienemann, C. P.; Carrier, H.; Grassl,  
401 B.; Bouyssiere, B.; Lobinski, R. Multielement molecular size fractionation in crude oil and oil  
402 residue by size exclusion microchromatography with high resolution inductively coupled plasma  
403 mass spectrometric detection (HR ICP MS). *J. Anal. At. Spectrom.* **2010**, *25* (12), 1974–1977.
- 404 (14) Gascon, G.; Vargas, V.; Feo, L.; Castellano, O.; Castillo, J.; Giusti, P.; Acavedo, S.;  
405 Lienemann, C.-P.; Bouyssiere, B. Size distributions of sulfur, vanadium, and nickel compounds  
406 in crude oils, residues, and their saturate, aromatic, resin, and asphaltene fractions determined by  
407 gel permeation chromatography inductively coupled plasma high-resolution mass spectrometry.  
408 *Energy Fuels* **2017**, *31* (8), 7783–7788.

- 409 (15) Gutierrez Sama, S.; Desprez, A.; Krier, G.; Lienemann, C.-P.; Barbier, J.; Lobinski, R.;  
410 Barrere-Mangote, C.; Giusti, P.; Bouyssiere, B. Study of the aggregation of metal complexes  
411 with asphaltenes using gel permeation chromatography inductively coupled plasma high-  
412 resolution mass spectrometry. *Energy Fuels* **2016**, *30* (9), 6907–6912.
- 413 (16) Desprez, A.; Bouyssiere, B.; Arnaudguilhem, C.; Krier, G.; Vernex-Loiset, L.; Giusti, P.  
414 Study of the size distribution of sulfur, vanadium, and nickel compounds in four crude oils and  
415 their distillation cuts by gel permeation chromatography inductively coupled plasma high-  
416 resolution mass spectrometry. *Energy Fuels* **2014**, *28* (6), 3730–3737.
- 417 (17) Caumette, G.; Lienemann, C. P.; Merdrignac, I.; Paucot, H.; Bouyssiere, B.; Lobinski, R.  
418 Sensitivity improvement in ICP MS analysis of fuels and light petroleum matrices using a  
419 microflow nebulizer and heated spray chamber sample introduction. *Talanta* **2009**, *80* (2), 1039–  
420 43.
- 421 (18) Vargas, V.; Castillo, J.; Torres, R. O.; Bouyssiere, B.; Lienemann, C.-P. Development of a  
422 chromatographic methodology for the separation and quantification of V, Ni and S compounds in  
423 petroleum products. *Fuel Process. Technol.* **2017**, *162*, 37–44.
- 424 (19) Huc, A.-Y. *Heavy Crude Oils*; IFP Publications, 2011.
- 425 (20) Gascon, G.; Negrin, J.; Garcia-Montoto, V.; Acevedo, S.; Lienemann, C.-P.; Bouyssiere,  
426 B. Simplification of heavy matrices by liquid–liquid extraction: part I—how to separate LMW,  
427 MMW, and HMW compounds in maltene fractions of V, Ni, and S compounds. *Energy Fuels*  
428 **2019**, *33* (3), 1922–1927.

429 (21) Gascon, G.; Negrín, J.; Montoto, V. G.; Acevedo, S.; Lienemann, C.-P.; Bouyssiere, B.  
430 Simplification of heavy matrices by liquid–solid extraction: part II—how to separate the LMW,  
431 MMW, and HMW compounds in asphaltene fractions for V, Ni, and S compounds. *Energy Fuels*  
432 **2019**, *33* (9), 8110–8117.

433

434 **TABLE CAPTIONS**

435 **Table 1.** Operating Conditions of the Pilot Plant Tests

436 **Table 2.** Feed Properties

437 **Table 3.** Results of Study A (Influence of the Temperature)

438 **Table 4.** Results of Study B (Influence of the Initial Deactivation Due to Coke Laydown)

439 **Table 5.** Slopes and Regression Coefficients for the Variation in V, Ni and S Concentrations vs.  
440 Temperature

441 **Table 6.** Slopes and Regression Coefficients for the Variation in V, Ni and S Concentration vs.  
442 Run Time (Hours)

443

444 **FIGURE CAPTIONS**

445 **Figure 1.** GPC ICP HR MS chromatograms of the V, Ni and S species in the atmospheric  
446 residue feedstock (ATM, green line), vacuum residue feedstock (VAC, blue line), blend of 93  
447 vol% ATM and 7% VAC (physical blend, red line) and theoretically reconstructed blend of 93  
448 vol% ATM and 7 vol% VAC (black dashed line) based on individual ATM and VAC  
449 chromatograms.

450 **Figure 2.** GPC ICP HR MS chromatograms of the V, Ni and S species in the feed (black dashed  
451 line) and product after hydrotreatment at different temperatures (the hydrotreatments at 375 °C,  
452 380 °C and 385 °C correspond to the blue, green and red lines, respectively).

453 **Figure 3.** The concentrations of V, Ni and S (total in black, HMW in blue, MMW in orange and  
454 LMW in gray) in the products that were hydrotreated at different temperatures quantified based  
455 on the total concentration and the GPC ICP HR MS chromatograms.

456 **Figure 4.** GPC ICP HR MS chromatograms of the V, Ni and S species in the feed (black dashed  
457 line) and the product for different run times after having been hydrotreated at the same  
458 temperature (the run times of 23 h, 52 h, 76 h and 100 h correspond to the light blue, red, green  
459 and blue lines, respectively).

460 **Figure 5.** The concentrations of V, Ni and S (total in black, HMW in blue, MMW in orange and  
461 LMW in gray) in the products that were hydrotreated for different run times quantified based on  
462 the total concentration and the GPC ICP HR MS chromatograms.

463